# Energy scale calibration of the ATLAS liquid argon electromagnetic calorimeter with $Z \rightarrow ee$ events.

CLHCP workshop, 25-28 Nov 2021, Nanjing

Hicham ATMANI

# OutLine

## Calibration of the electromagnetic calorimeter of the ATLAS detector.

1. Introduction :
    - Motivation
    - Calibration procedure
2. Electron energy calibration :
    - Energy scale factors
    - Additional constant term
3. Low pile-up runs calibration :
    - Extrapolation study
    - Extrapolation systematics
4. Conclusion.

# Motivation:

- **Electromagnetic particles are heavily used in precision measurements due to the high precision reachable by the electromagnetic (EM) calorimeter.**

**Measuring the mass of the W boson with an uncertainty less than 19 MeV**

arXiv:1701.07240

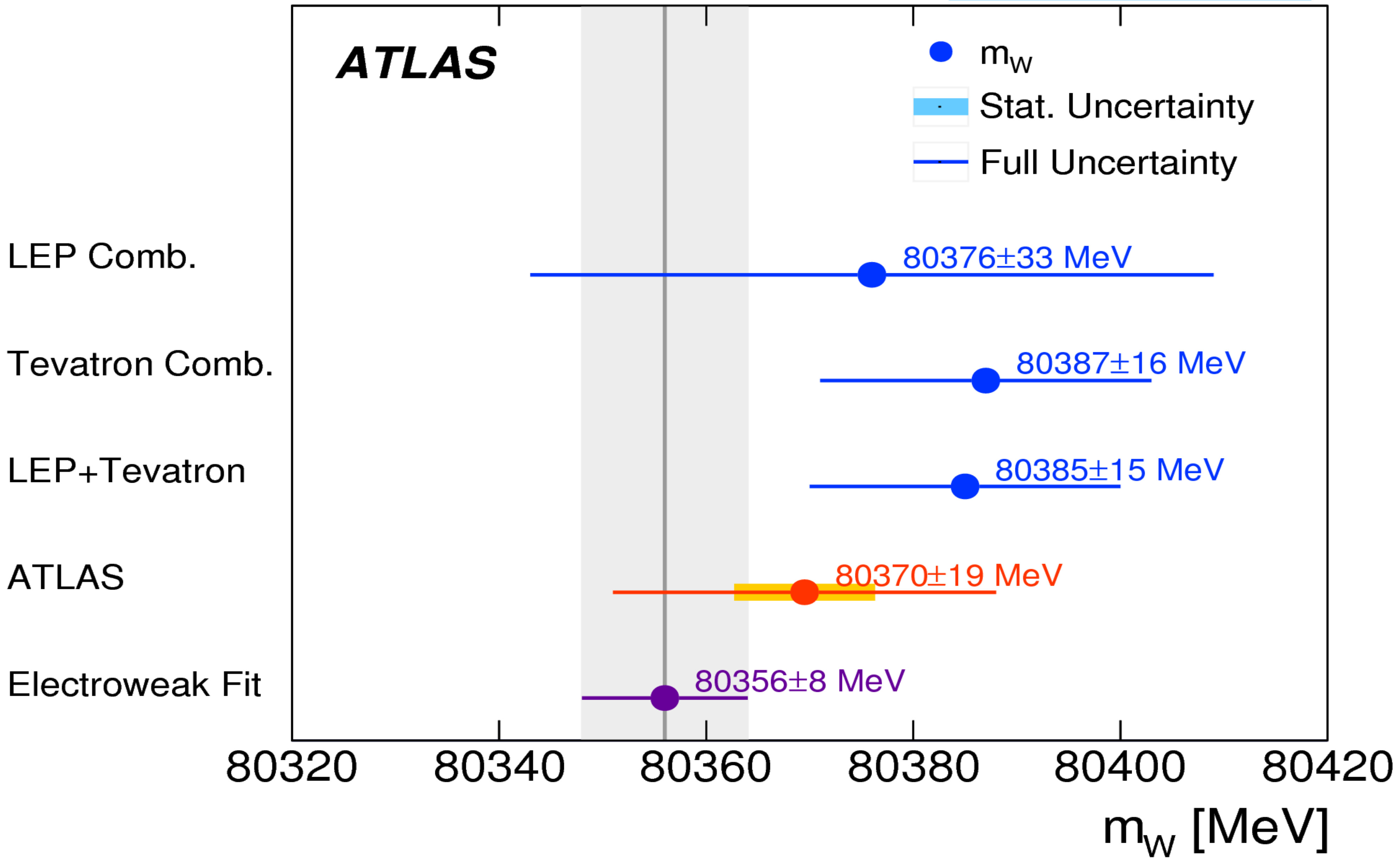


$$m_W = 80370 \pm 7\ (\text{stat.}) \pm 11\ (\text{exp. syst.}) \pm 14\ (\text{mod. syst.})\ \text{MeV}$$
$$= 80370 \pm 19\ \text{MeV},$$

**The measurement of the properties of the Higgs boson ($H \rightarrow \gamma\gamma$ and $H \rightarrow 4l$ )**

arXiv:1806.00242

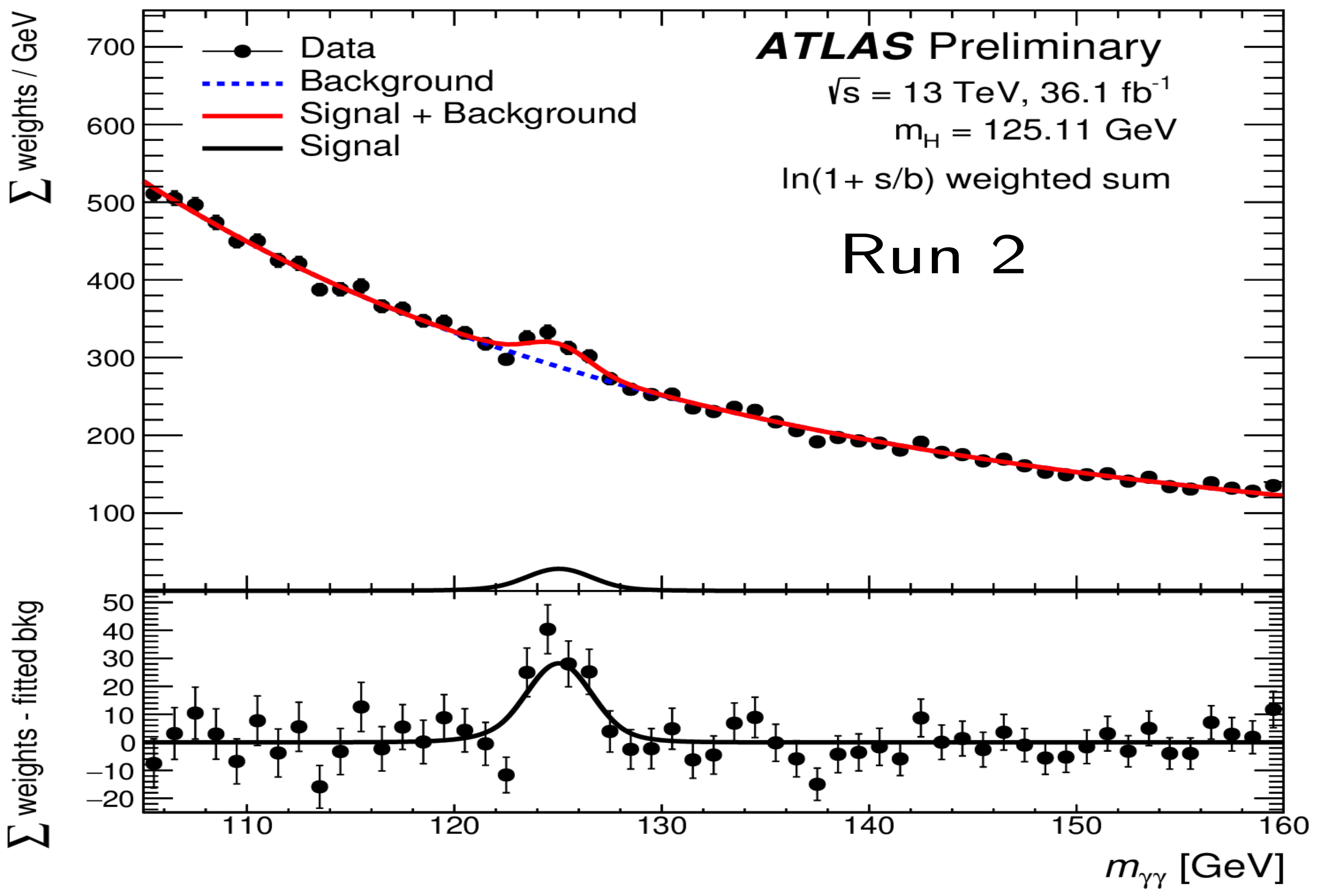


| Channel | Mass measurement [GeV] |
|---|---|
| $H \rightarrow \gamma\gamma$ | $125.98 \pm 0.42(\text{stat}) \pm 0.28(\text{syst}) = 125.98 \pm 0.50$ |
| $H \rightarrow ZZ^* \rightarrow 4\ell$ | $124.51 \pm 0.52(\text{stat}) \pm 0.06(\text{syst}) = 124.51 \pm 0.52$ |
| Combined | $125.36 \pm 0.37(\text{stat}) \pm 0.18(\text{syst}) = 125.36 \pm 0.41$ |

***To reach a high precision in property measurements, a precise calibration of the energy of electrons and photons is required.***

# Calibration procedure:

Steps 1 to 4:

- The EM clusters are calibrated to the energy in simulation using multivariate techniques.
- The EM calorimeter is longitudinally segmented : Equalise scales of different longitudinal layers between data/Simulation.

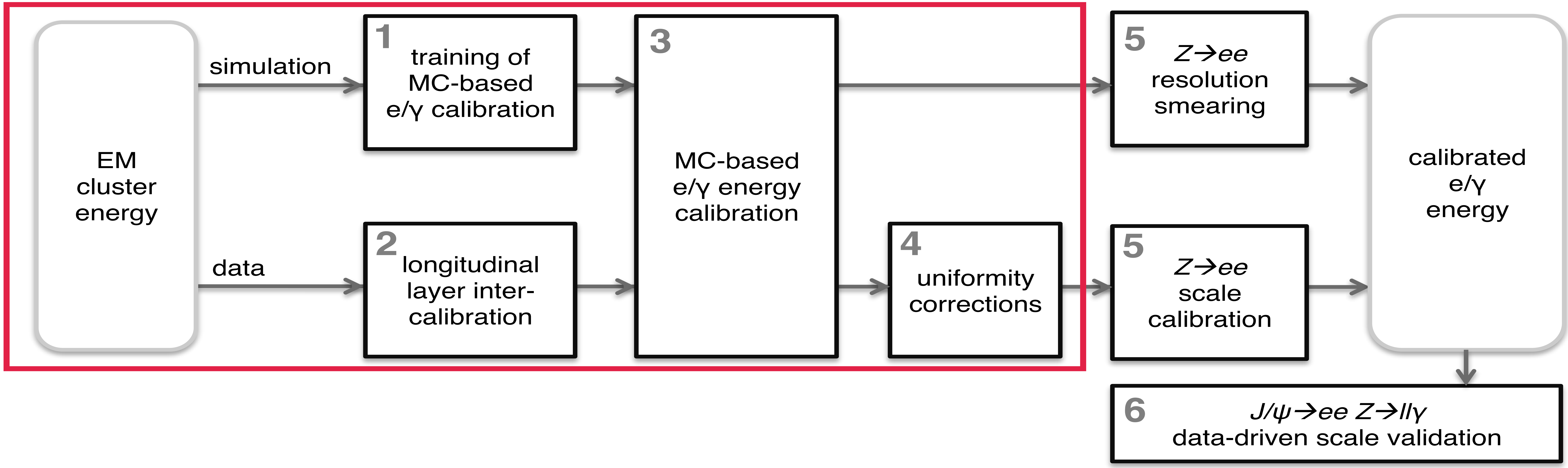

# Calibration procedure:

- Step 4: An important difference between data and simulation:

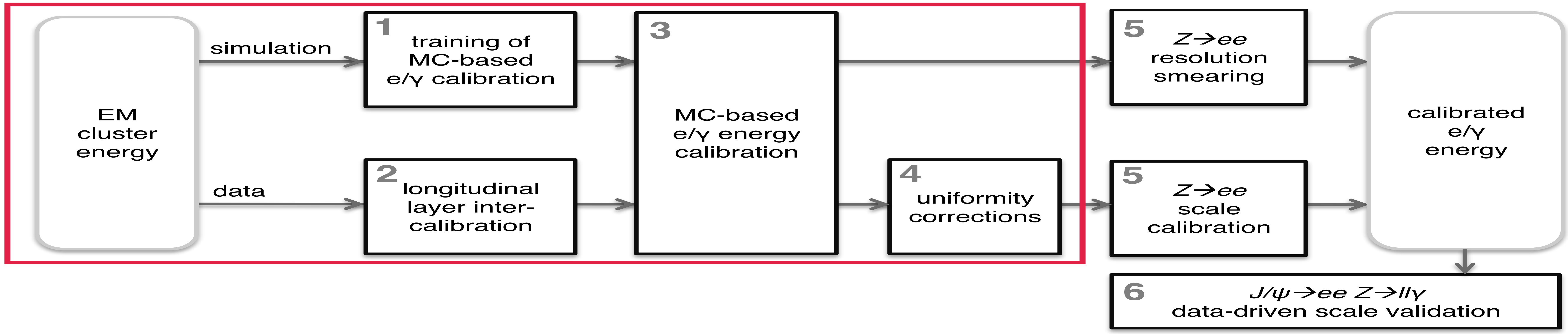


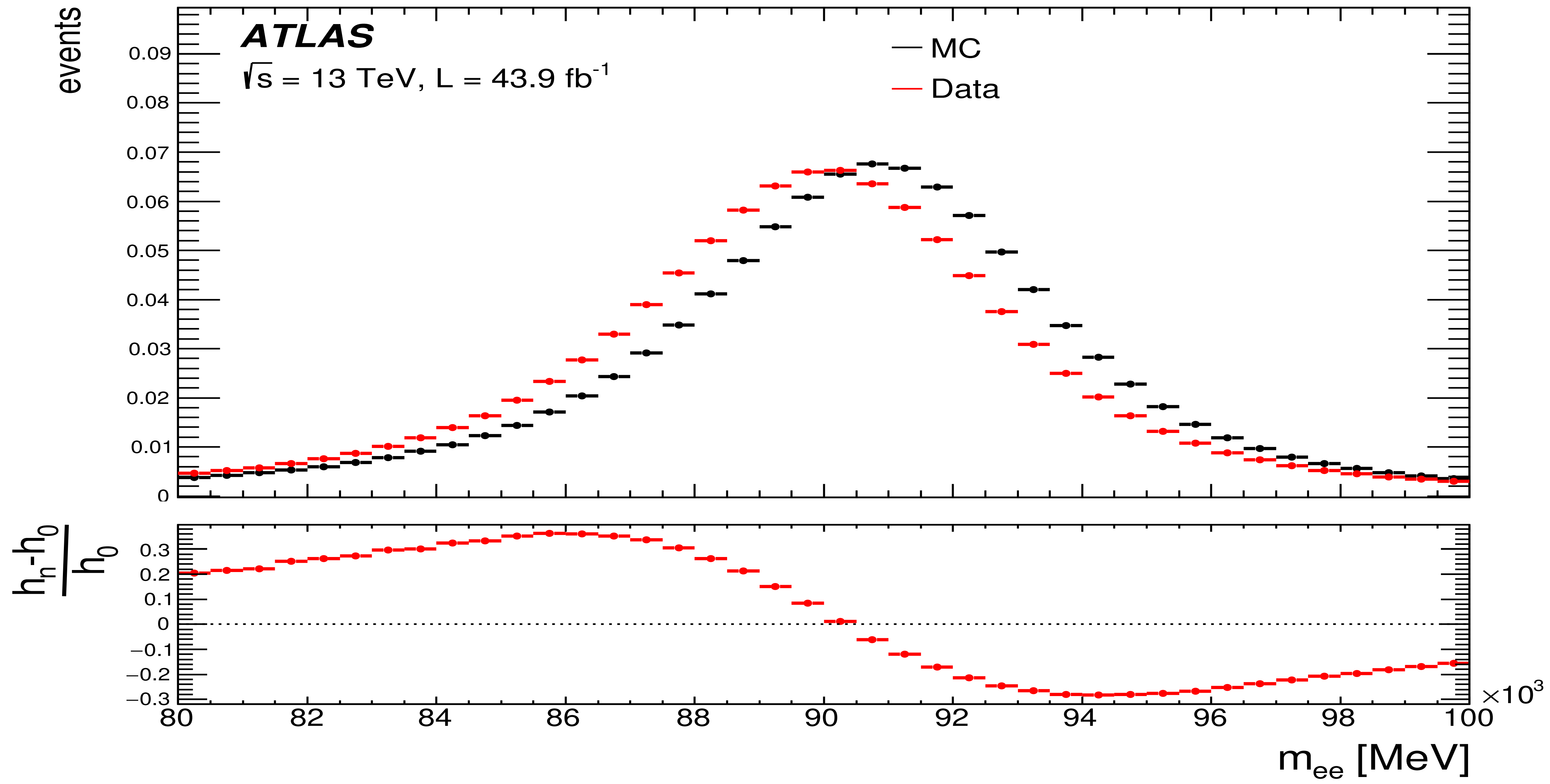


- Di-electron invariant mass $m_{ee}$ at the step 4 of the calibration procedure:

$$m_{\mathrm{ee}} = \sqrt{2E_1 E_2\,(1 - \cos\theta_{12})}, \qquad (2)$$

- The difference between data and simulation is corrected in step 5 (next slide, one of the main activities of the thesis).

# Calibration procedure:

- Step 5: Two correction factors are extracted and applied to data and simulation.

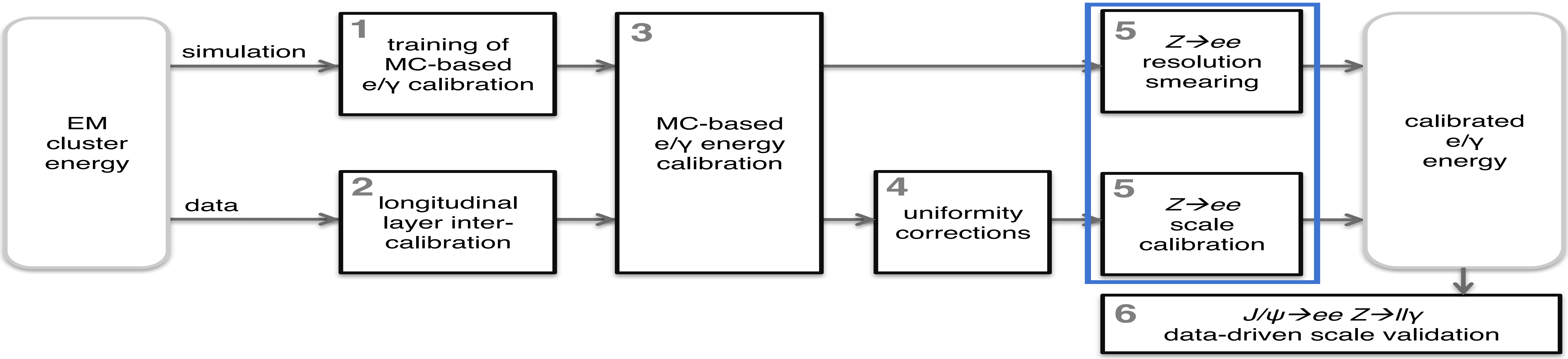


- The energy scale factor $\alpha$:

$$E_i^{\text{corr}} = \frac{E_i^{\text{data}}}{1+\alpha_i}$$

- Applied to the data in order to match the energy response of the simulation.

- The additional constant term $c'$:

$$\left(\frac{\sigma(E)}{E}\right)_i^{\text{corr}} = \left(\frac{\sigma(E)}{E}\right)_i^{\text{MC}} \oplus c'_i$$

- Applied to the simulation to be in agreement with the energy resolution of the data.

# Calibration of the EM calorimeter: Results

**JINST 14 (2019) P12006**

**Energy scale correction $\alpha$**

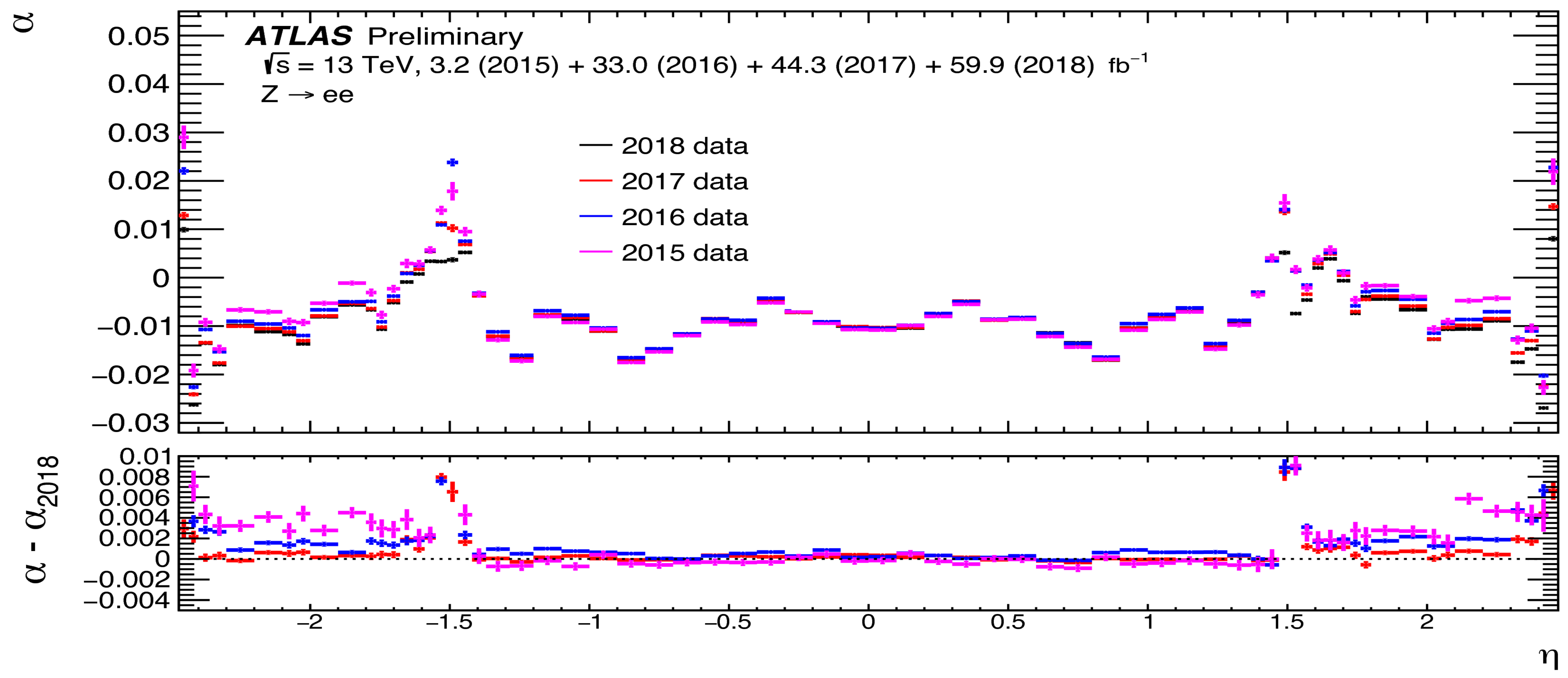


- The difference observed in the end-cap region is related to the difference of instantaneous luminosity.
- The difference of instantaneous luminosity affects the HV drop and temperature.

**JINST 14 (2019) P12006**

**Resolution correction $c'$**

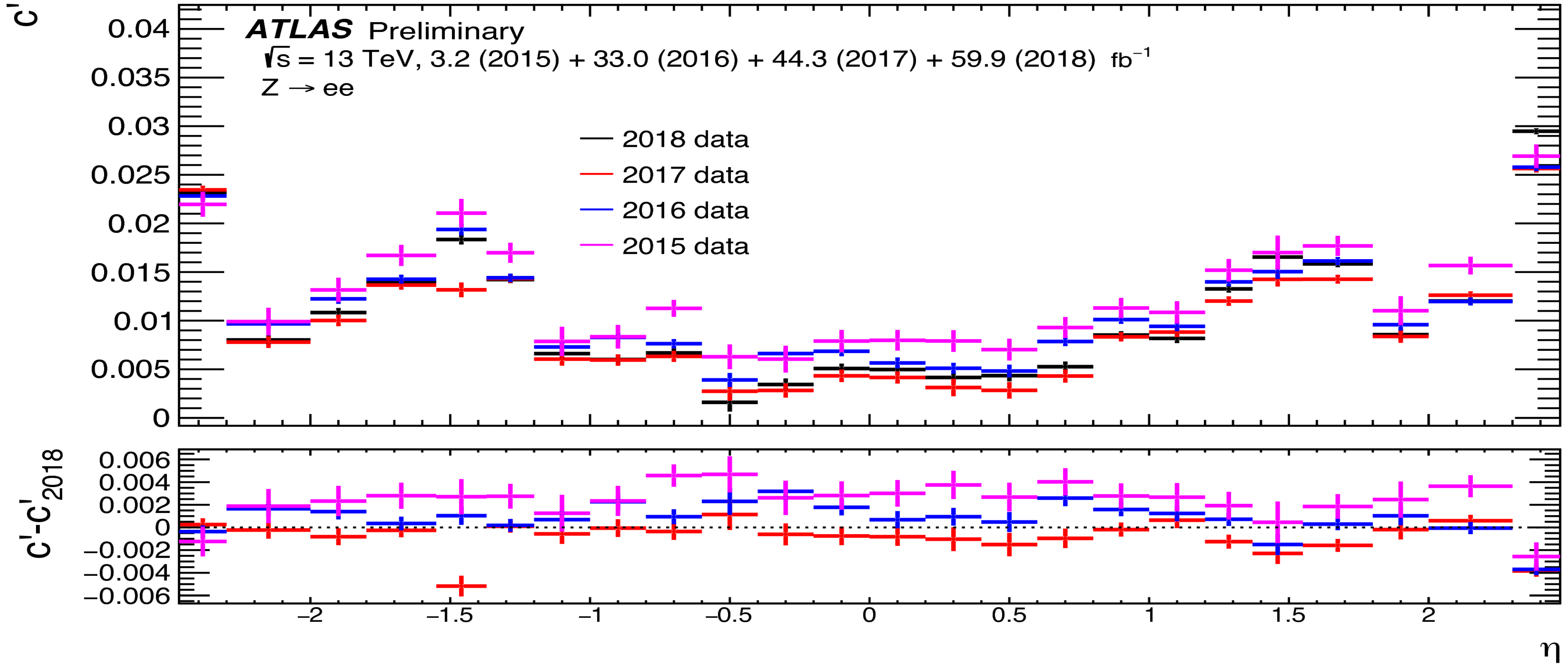


- The derived effective constant terms depend on the year i.e on the pileup (lower values for 2017 than 2016).
- This effect is explained by an overestimation of the pileup noise in the simulation.

# Calibration of the EM calorimeter: Conclusion

JINST 14 (2019) P12006

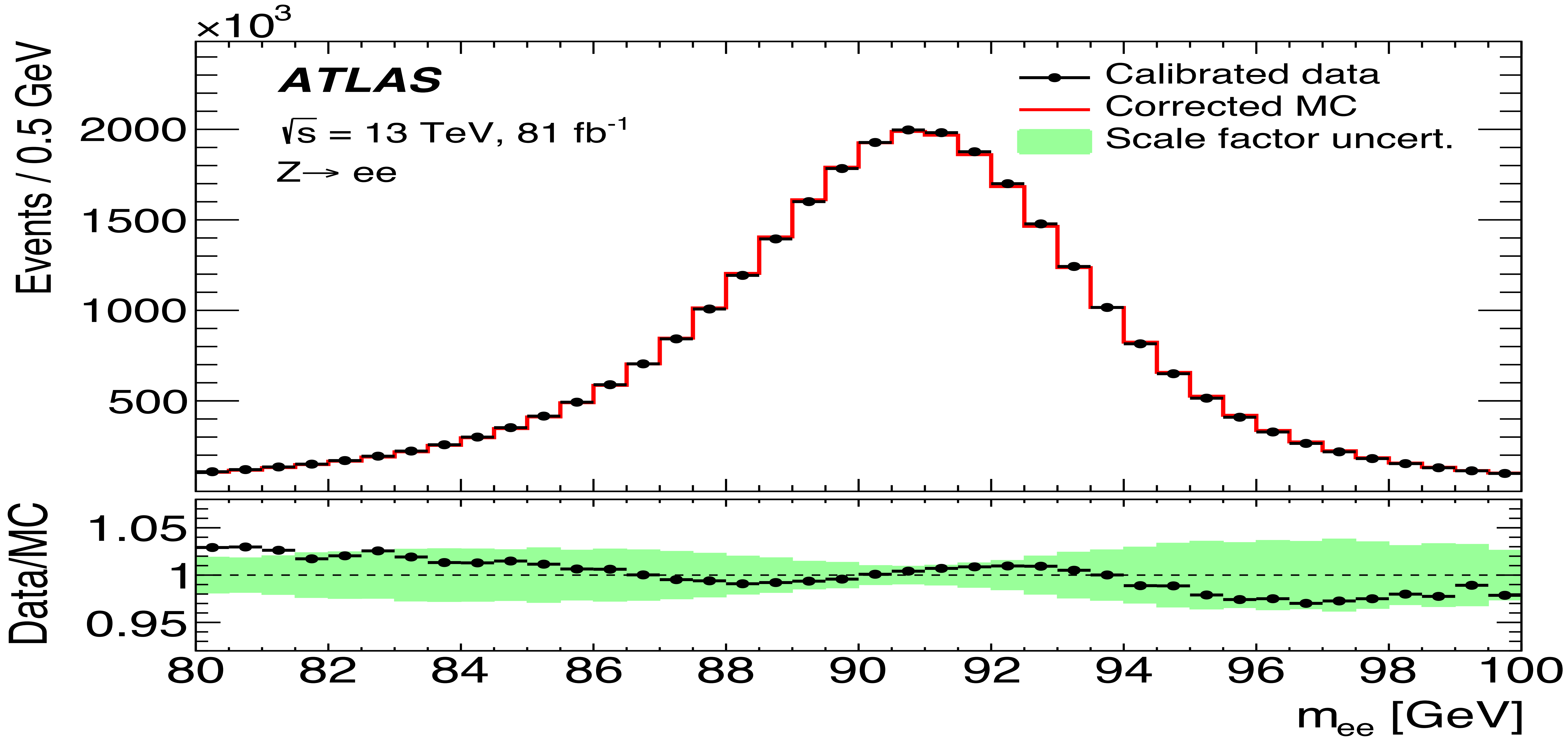


**Uncertainty sources:**

Method accuracy
Method comparison
Mass range
Region selection
Bkg. with prompt electrons
Electron isolation requirement
Electron identification criteria
Electron bremsstrahlung removal
Electron efficiency corrections

- Inclusive di-electron invariant mass distribution from $Z \rightarrow ee$ decays in data compared to MC after applying the full calibration.
- The lower panel shows the data to simulation ratio, together with the uncertainty from the energy scale and resolution corrections.

# Calibration of low pileup runs

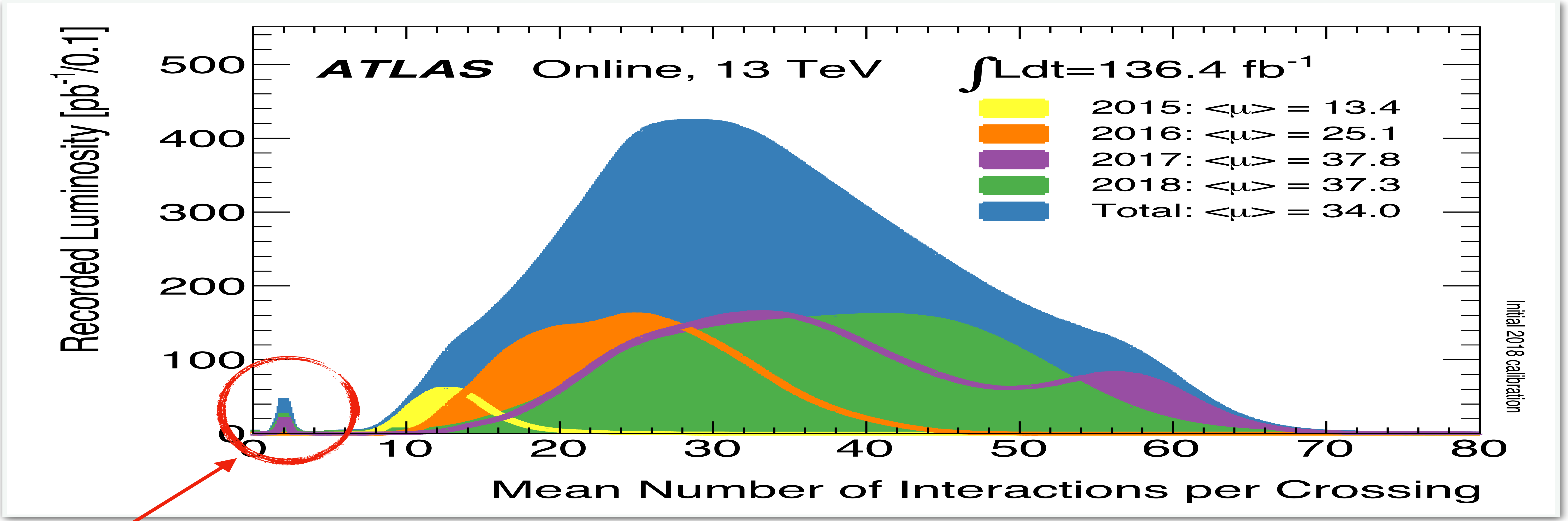


Low pileup dataset

- Due to the limited statistics of the low pileup datasets
  - The same procedure is applied with fewer number of $\eta$ bins.
  - An extrapolation from the nominal pileup datasets is performed as an alternative approach.

# Extrapolation approach

**JINST 14 (2019) P12006**

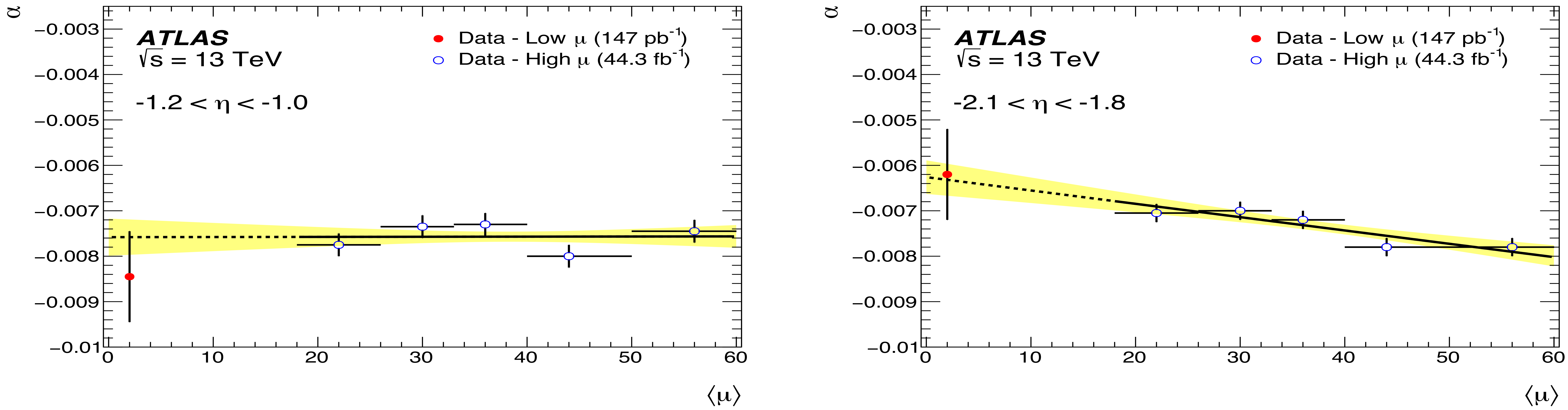


- The blue points show the energy scale $\alpha$ for the high pileup dataset as a function of $\langle \mu \rangle$.
- The black lines show the extrapolation to $\langle \mu \rangle \approx 2$ using a linear function and five intervals of $\langle \mu \rangle$.
- The band represents the uncertainty in the extrapolation.
- The extrapolation results are compared with the energy scale factors extracted from the low pileup dataset, represented by the red point.

# Calibration of low pileup runs: Conclusion

JINST 14 (2019) P12006

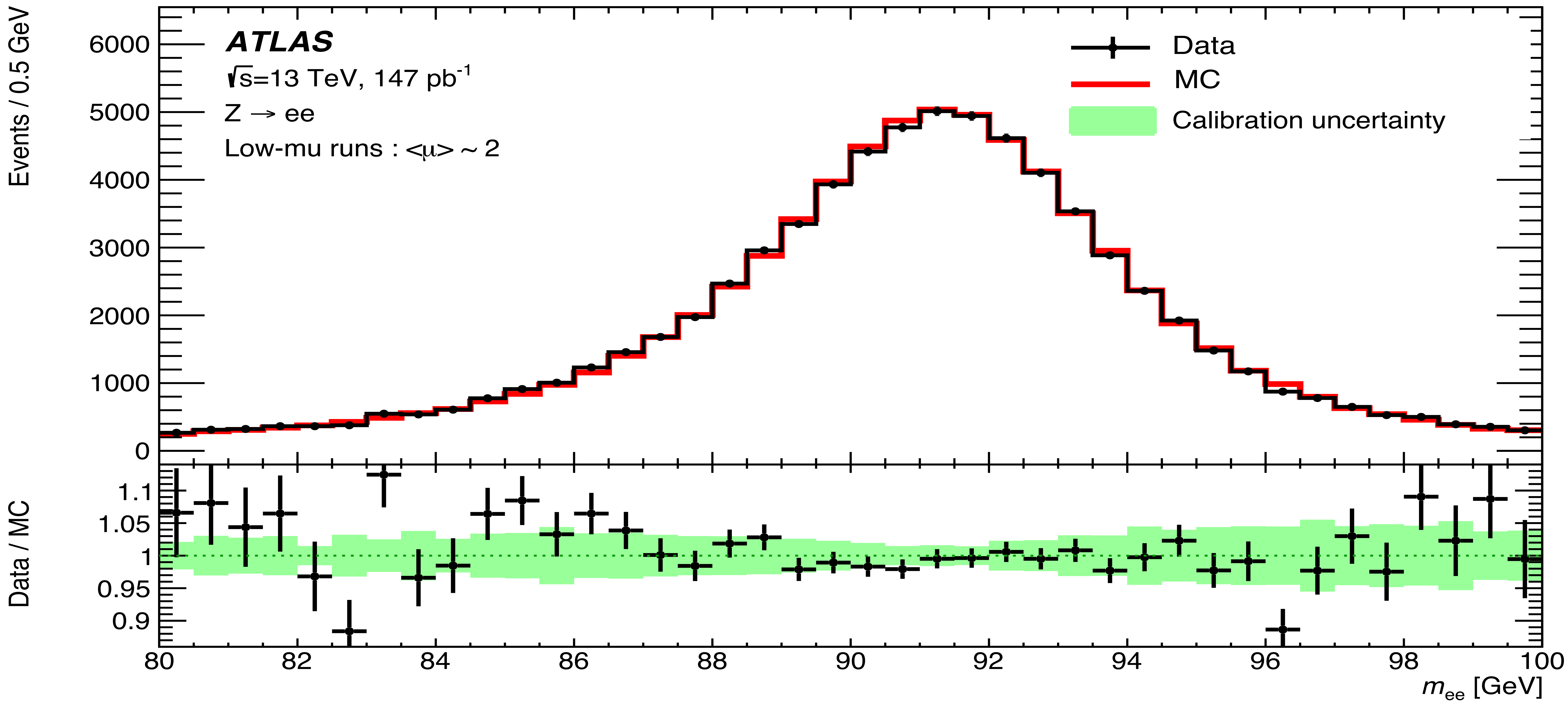


- Inclusive di-electron invariant mass distribution from $Z \to ee$ decays in data compared to MC after applying the full calibration for the low pileup runs.
- The lower panel shows the data to simulation ratio, together with the statistical uncertainty.

# Summary

## Calibration of standard runs

- A difference between data and simulation is observed in the calibration of ATLAS electromagnetic calorimeter.
- I worked on the extraction of two scale factors ($\alpha$, $c'$), used to correct this difference.
- The results presented in this thesis are used by the ATLAS collaboration for the standard Run 2 dataset.

## Calibration of low pileup runs

- The same difference is observed also for low pileup runs.
- I used an alternative approach to correct the difference between data and simulation.
- The alternative approach consists of extrapolating the scale factors from the standard to the low pileup runs.

# Backup

# LHC datasets:

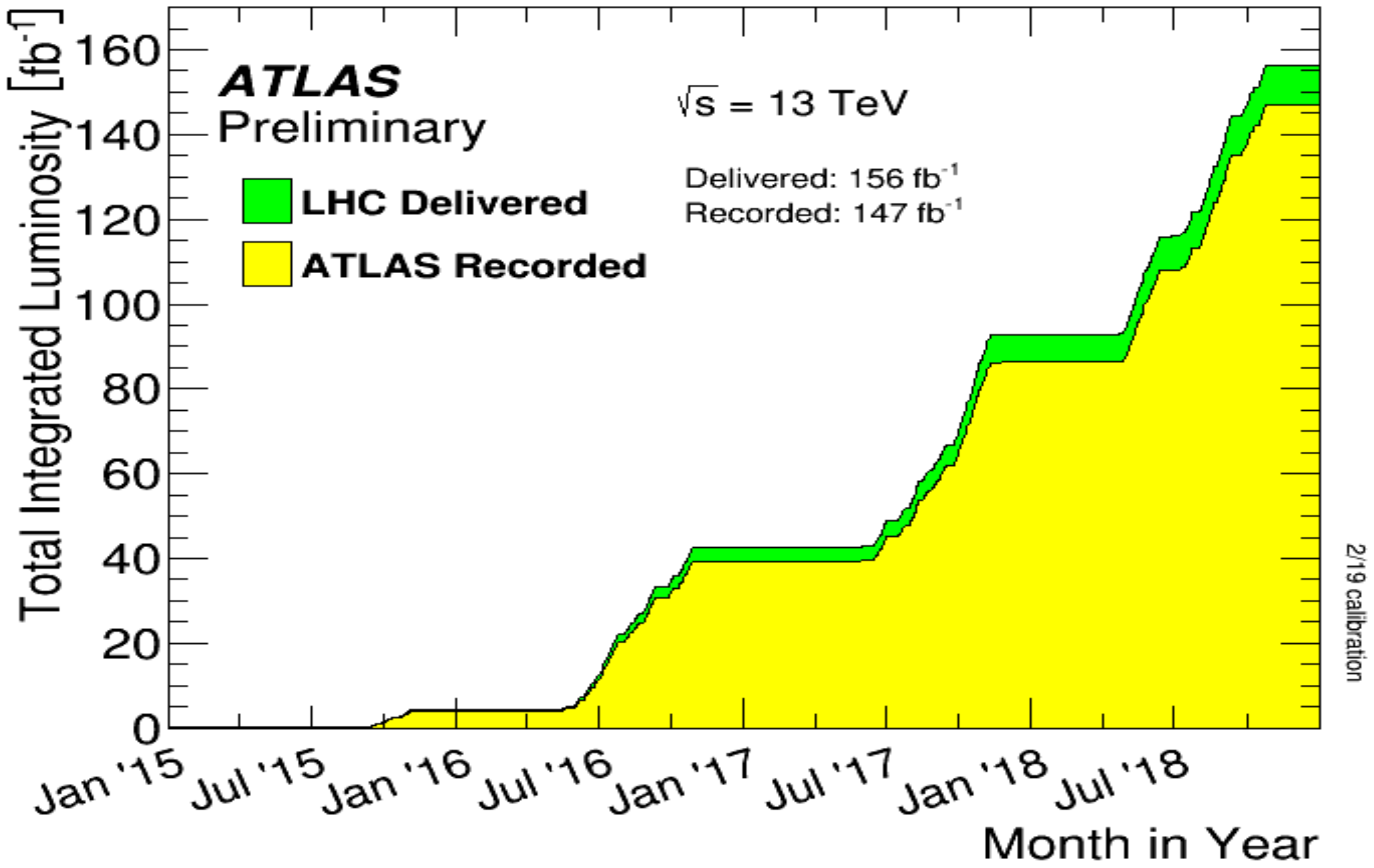


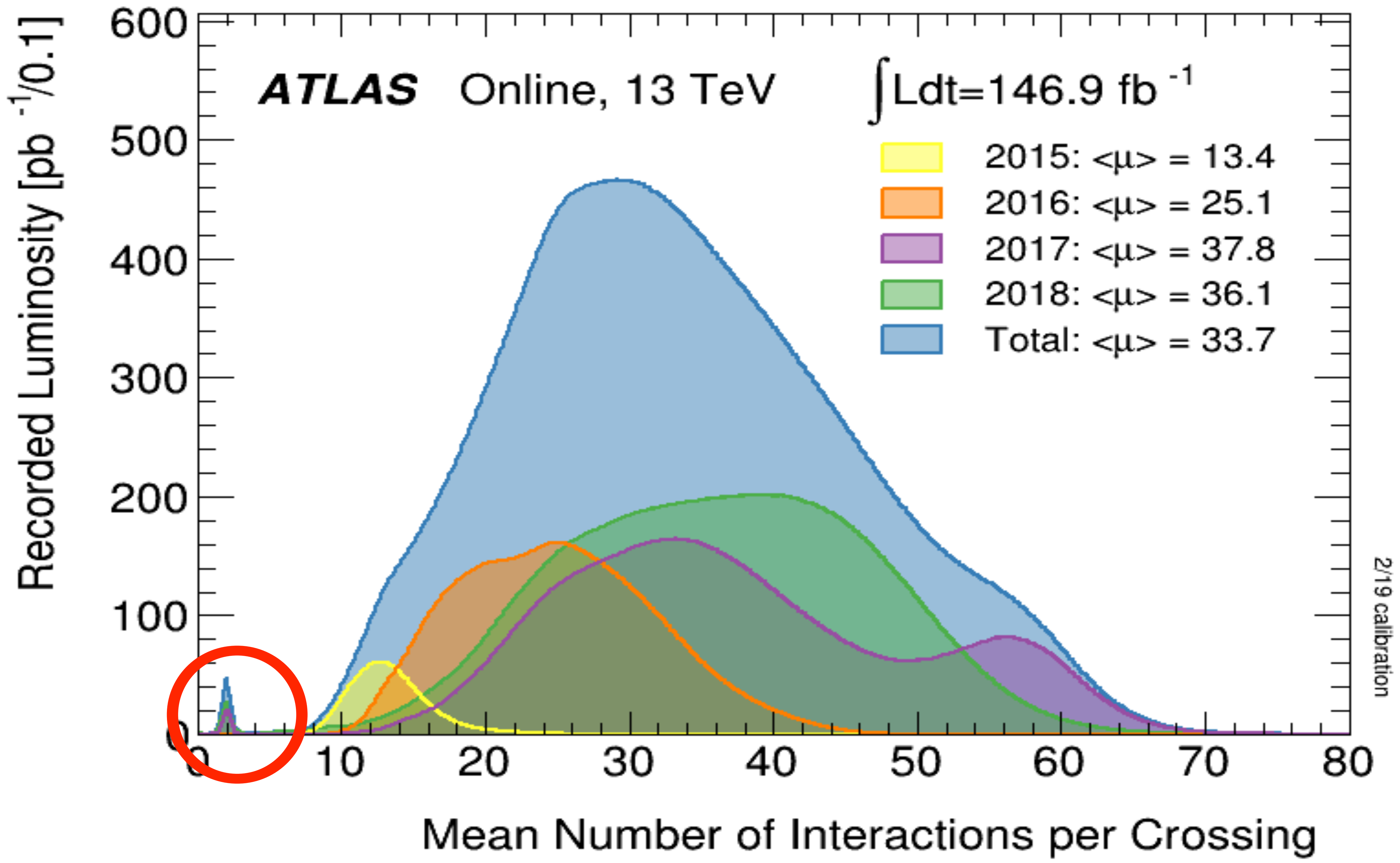


- Run 1: 2010 $\rightarrow$ 2012, (7 and 8 TeV)
- Run 2: 2015 $\rightarrow$ 2018, (13 TeV)
- The integrated luminosity:

$$L_{\text{int}} = \frac{N_{\text{process}}}{\sigma_{\text{process}}}.$$

- Total integrated luminosity at Run 2 correspond to 147 $\text{fb}^{-1}$ ($\times$ 7 Run 1).

- Recorded luminosity as a function of the number of interactions per crossing.
- Special runs are collected at ($\mu \approx 2$), correspond to 599 $\text{pb}^{-1}$ at 5 and 13 TeV.
- low pile-up runs are used for precision measurements.

# Calibration procedure:

## The correction factors $\alpha_i$ and $c'$ are:

- Extracted from the Z $\rightarrow$ ee channel, by comparing invariant mass $m_{ee}$ distributions.
- Extracted in bin of $\eta_{\text{calo}}$: 68 and 24 bins are used respectively for $\alpha$ and $c'$.
- Extracted using the template method.

The template method is used to measure $\alpha_i$ and $c'$ simultaneously.

- Create distorted MC (Template) with known values of $\alpha_i$ and $c'$.
- Compute $\chi^2$ between $Z$ mass distributions of date and the template.
- Fit the minimum of the $\chi^2$ distribution in the ($\alpha_i$,$c'$ ) plan.

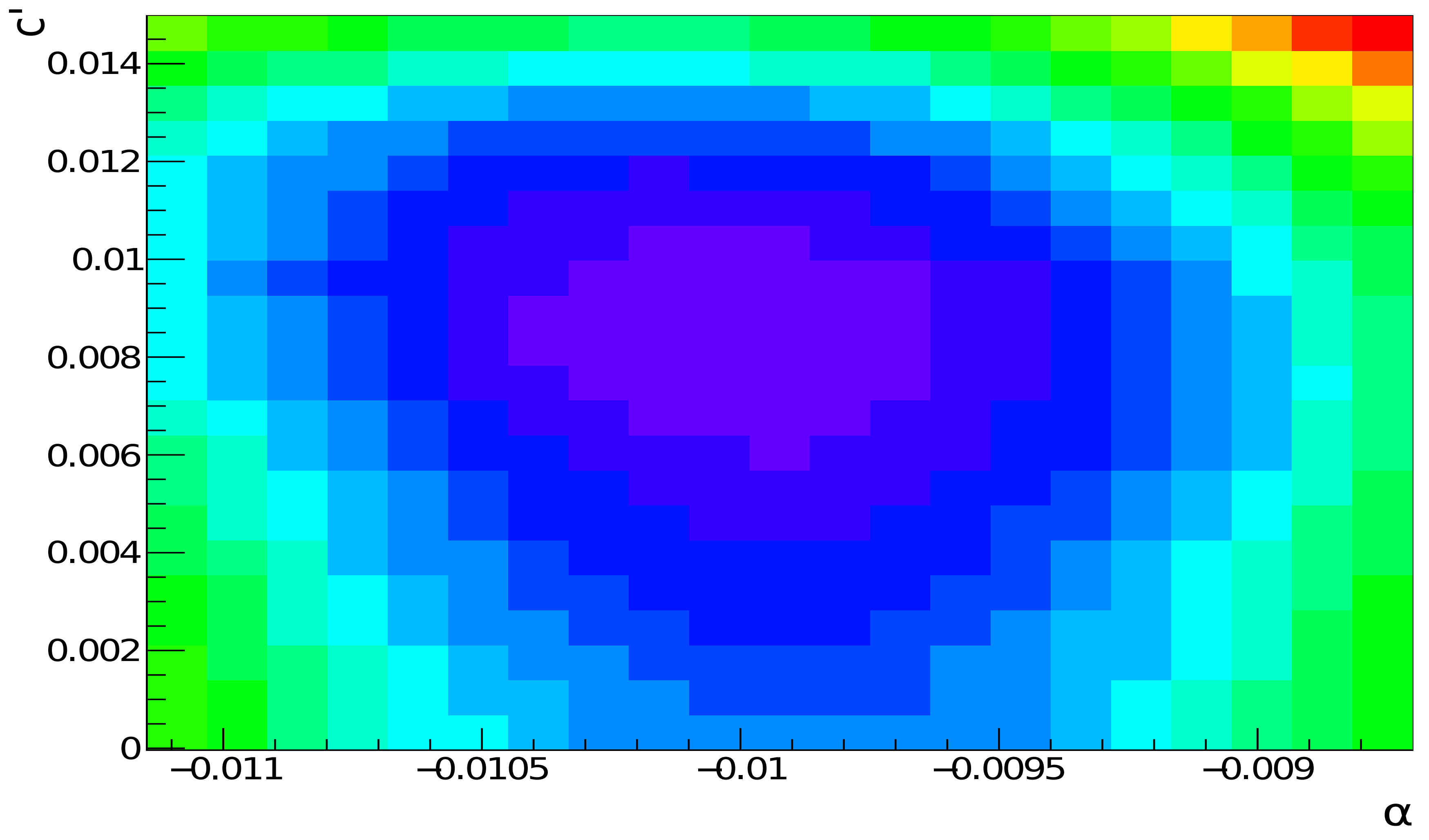


Several 1D fits are performed to determine the minimum of $\chi^2$, corresponding to the best agreement between the template and data.

# Extrapolation results

**JINST 14 (2019) P12006**

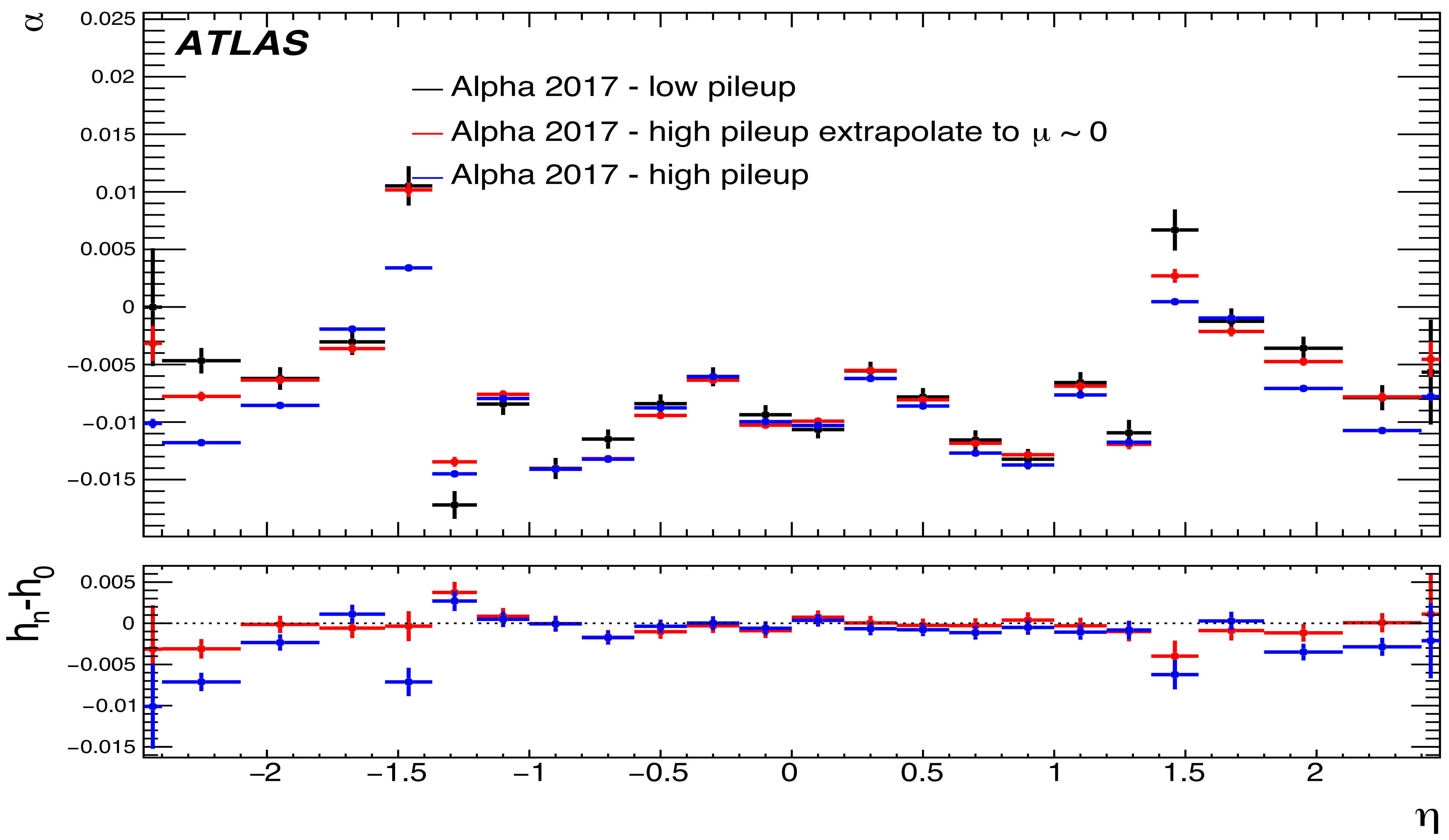


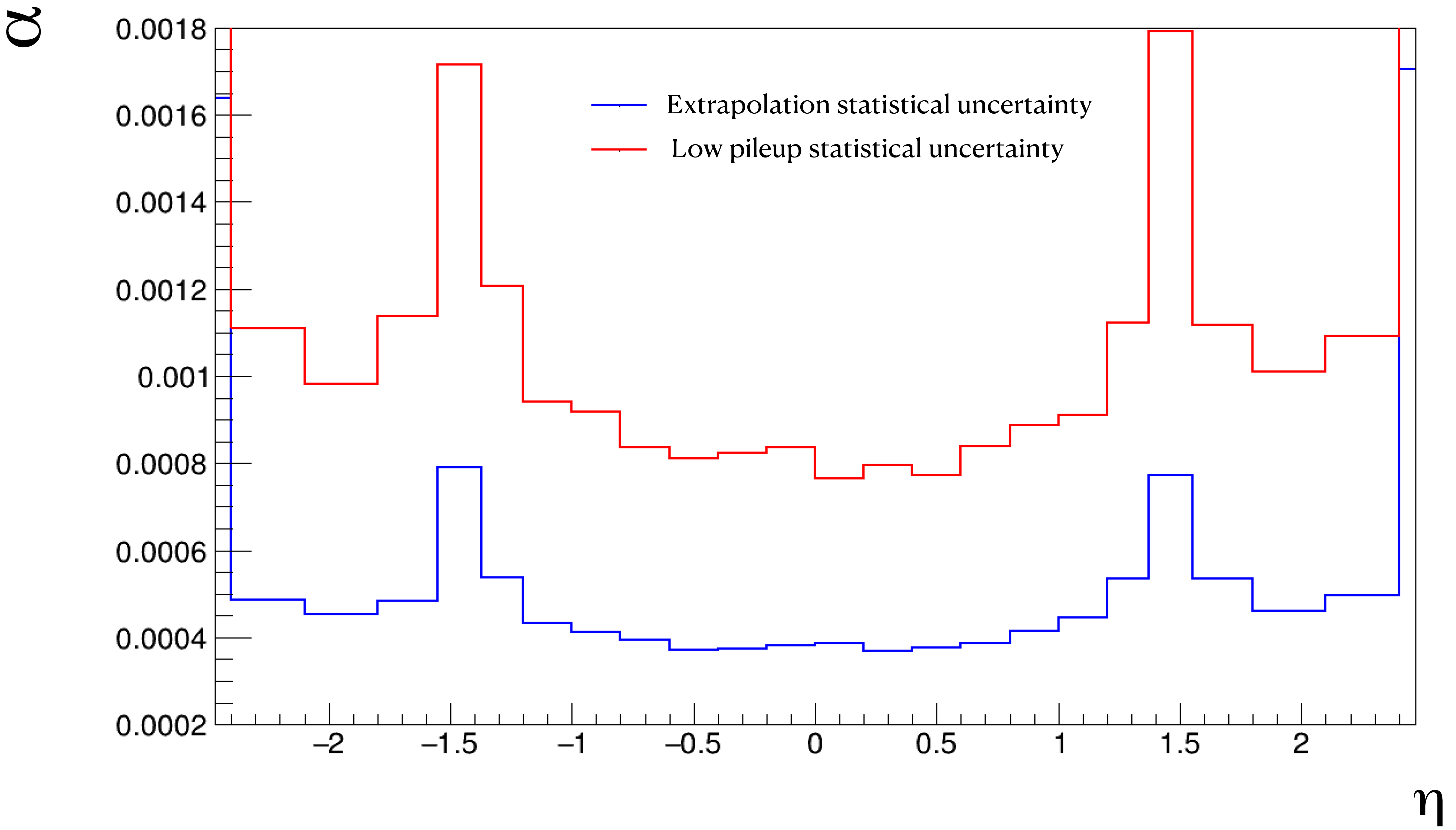


- Except for the transition region, the extrapolation results are similar to low pile-up results.
- The extrapolation results allow to reduce the statistical uncertainty.

# Uncertainties on the extrapolation approach:

- The different sources of uncertainties are classified as below:

- High pileup uncertainties.
- Extrapolation uncertainties.
- Temperature uncertainties.

- Threshold difference uncertainties.
- Extrapolation statistical uncertainty.

**JINST 14 (2019) P12006**

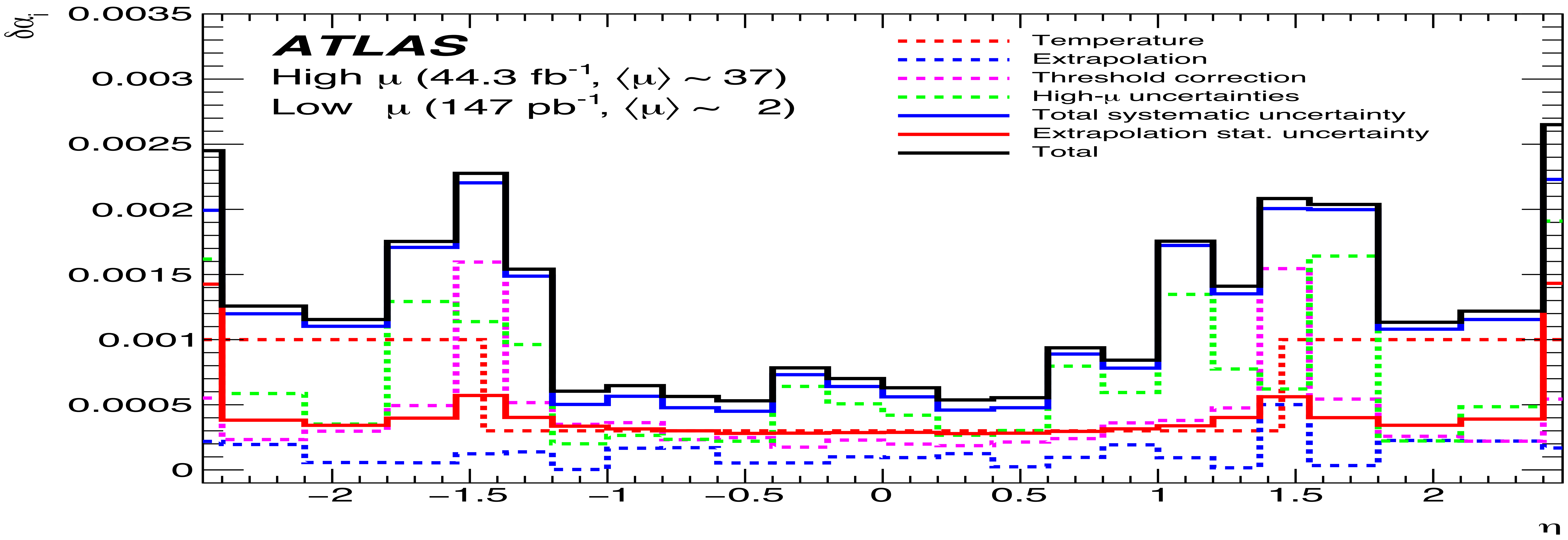

# Backup: pileup modeling

- **Nominal**: resolution correction term for 2017 dataset.
- **pileup**: resolution correction term for 2017 dataset after correcting the pileup overestimation problem.

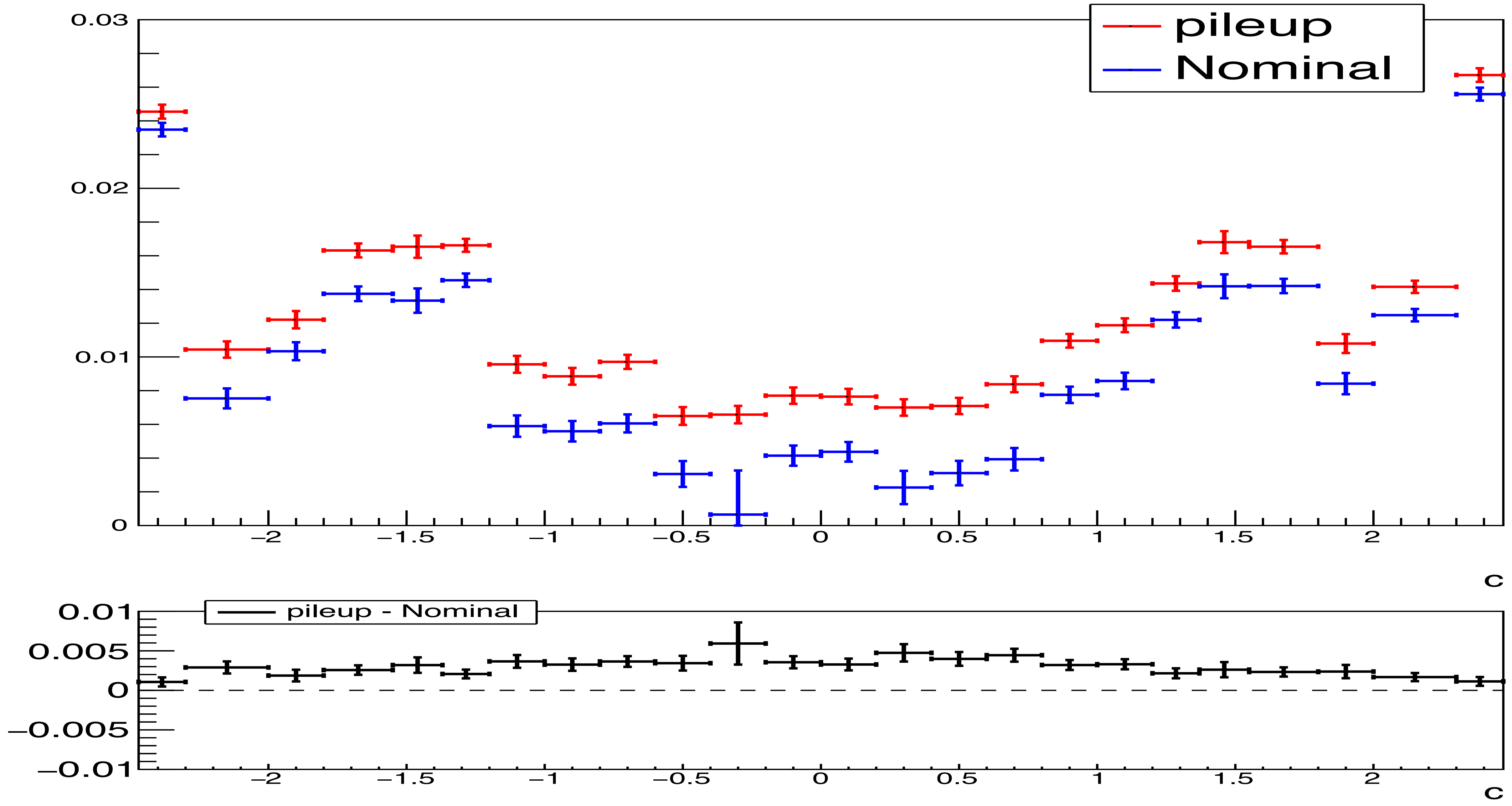


- After correcting the pileup modeling problem, 2017 results are higher and closer to 2015 results.

# Backup: Difference of threshold

- For high and low pile-up runs, we use different topo-cluster noise threshold for the energy reconstruction.
- The difference of threshold can be illustrated in the plot below : for the low pile-up data, the threshold for the energy reconstruction is lower ans thus more more energy is collected in the cluster and the reconst ucted invariant mass in higher on average.